NORSAR

NORSAR Scientific Report No. 1-88/89

Final Technical Summary

1 April – 30 September 1988

L.B. Loughran (ed.)

Kjeller, December 1988

VII.2   Statistics of ISC travel time residuals

The location of seismic events by a network of stations requires that adequate theoretical travel times are available, either by interpolation in tables, or by calculating the times in a reference velocity model. Despite obvious shortcomings the Jeffreys-Bullen tables are still in use at the major seismological centers for locating events. The more recent PREM model (Dziewonski and Anderson, 1981) is more satisfying in that it was constructed to fit a large seismological data set including free oscillation eigenfrequencies, but the original transversely isotropic model is not well suited for routine travel time calculations, and the isotropic version of PREM has not been adequately tested against arrival time observations. Here we report on the statistics of teleseismic travel time residuals with respect to the isotropic PREM.

We have extracted P arrival time data from the ISC bulletins for the year 1984, PcP and PKP for the years 1975-1984, and PKKP for the years 1964-1984. Additional PKKP and PnKP, n > 2, were taken from bulletins of the original LASA and NORSAR arrays, and from special publications. All data were subjected to a standard processing sequence, similar to that of others: Residuals were computed relative to PREM, subjected to station corrections, corrected for ellipticity and lower mantle variations, and corrected for the effects of source structure and/or mislocation. Data belonging to a particular branch were finally averaged to form 'summary ray' data, based on pairs of approximately equal area blocks (equalling 10 x 10° at the equator). For details of the data selection and processing we refer to Doornbos and Hilton (1988). The number of 'summary ray' data finally obtained were 5415 for P, 1668 for PcP, 1395 for PKP (13C), 871 for PKP (AB), 686 for PKKP (13C), and 189 for PnKP (AB).

Typical examples of histograms of summary residual data are shown in Fig. VII.2.1. In this figure we have also plotted the data from deep events. A comparison suggests that reading errors are significant especially for arrivals from shallow events; note that the number of

late readings is reduced in the data from deep events. For the core
phases and for P at distances larger than 85° (P2), the early parts of
the histograms for all data and for the data from deep events overlay
quite well. This means that the upper mantle model of PREM is consis-
tent with the ISC depth estimates. The P data at distances smaller than
85° (P1) are different in that there are anomalously many early
arrivals from shallow events; this may also explain the relatively
large variance of these data. It is possible that one begins to see
here the effect of subduction zones, since many of the events occur
within these zones.

Fig. VII.2.1 also shows that there is a significant mean residual left
in the data. This is especially clear for the core phases, and we can
infer their relation. If the sampling by summary rays is reasonably
uniform and if nonlinear effects can be neglected, then for any
particular phase the mean residual represents the effects of dif-
ferences between PREM and the spherically averaged earth, and/or
systematic reading errors. The PcP, PKP and PnKP mean residuals for
summary rays in the same ray parameter interval are expected to follow
a linear trend:

$$\overline{\delta T}(PnKP) = \overline{\delta T_m} + n\overline{\delta T_c}, \qquad n = 1,2,\ldots \qquad (1)$$

where $\overline{\delta T_m} \equiv \overline{\delta T}(PcP)$, and $\overline{\delta T_c}$ represents the residual after one passage
of the wave through the core; both the velocity structure and the core-
mantle boundary level may contribute to the residual. A relation of the
form (1) can be discerned for the phases with ray parameters above
4 s/d, but surprisingly, PcP, PKP and PKKP in the ray parameter range
2-3 s/d do not follow a linear trend. One possible explanation, now
under investigation, is based on the fact that PcP at small distances
is weak, and known to be often unobservable. It is therefore possible
that PcP (and possibly PKKP) is observed primarily in circumstances of
relatively strong focusing, with an accompanying phase delay.

It is also of interest to note that the variance of the PKKP data is not much larger than that of PKP in the same ray parameter range (2-3 s/d). It is convenient to plot the variance of the various phases as a function of their sensitivity to variations of deep earth structure. Here we give such a relation between the variance of the data σ_T^2 and the variance of core-mantle boundary topography σ_r^2. For PcP:

$$\sigma_T^2 = \sigma_o^2 + \frac{4}{r^2} \; (\eta^{+2}-p^2) \; \sigma_r^2 \tag{2a}$$

and for PnKP if the perturbations δr in the sampling points r_i are uncorrelated:

$$\sigma_T^2 = \sigma_o^2 + \frac{2}{r^2} \; [\{(\eta^{-2}-p^2)-(\eta^{+2}-p^2)^{1/2}\}^{1/2} + 2 \sum_{i=2}^{n} (\eta^{-2}-p^2)]\sigma_r^2 \tag{2b}$$

Here $\eta = r/v$, and a superscript $^+/^-$ refers to the top/bottomside of the boundary. In Fig. VII.2.3 the variance of the data subsets is plotted following equation (2). One inference from this figure is that the PKKP data imply a relatively smooth core-mantle boundary on a large scale; for illustrative purposes the expected travel time variance for $\sigma_r^2 = 1$ km^2 is shown in Fig. VII.2.3. Another inference is that models of large-scale lateral variation of deep earth structure can explain only a relatively small part of the data variance.

<div align="center">
D.J. Doornbos
T. Hilton
</div>

References

Doornbos, D.J. and T. Hilton (1988): Models of the core-mantle boundary and the travel times of internally reflected core phases, submitted for publication.

Dziewonski, A.M. and D.L. Anderson (1981): Preliminary Reference Earth Model (PREM). Phys. Earth Planet. Inter., 25, 297-356.
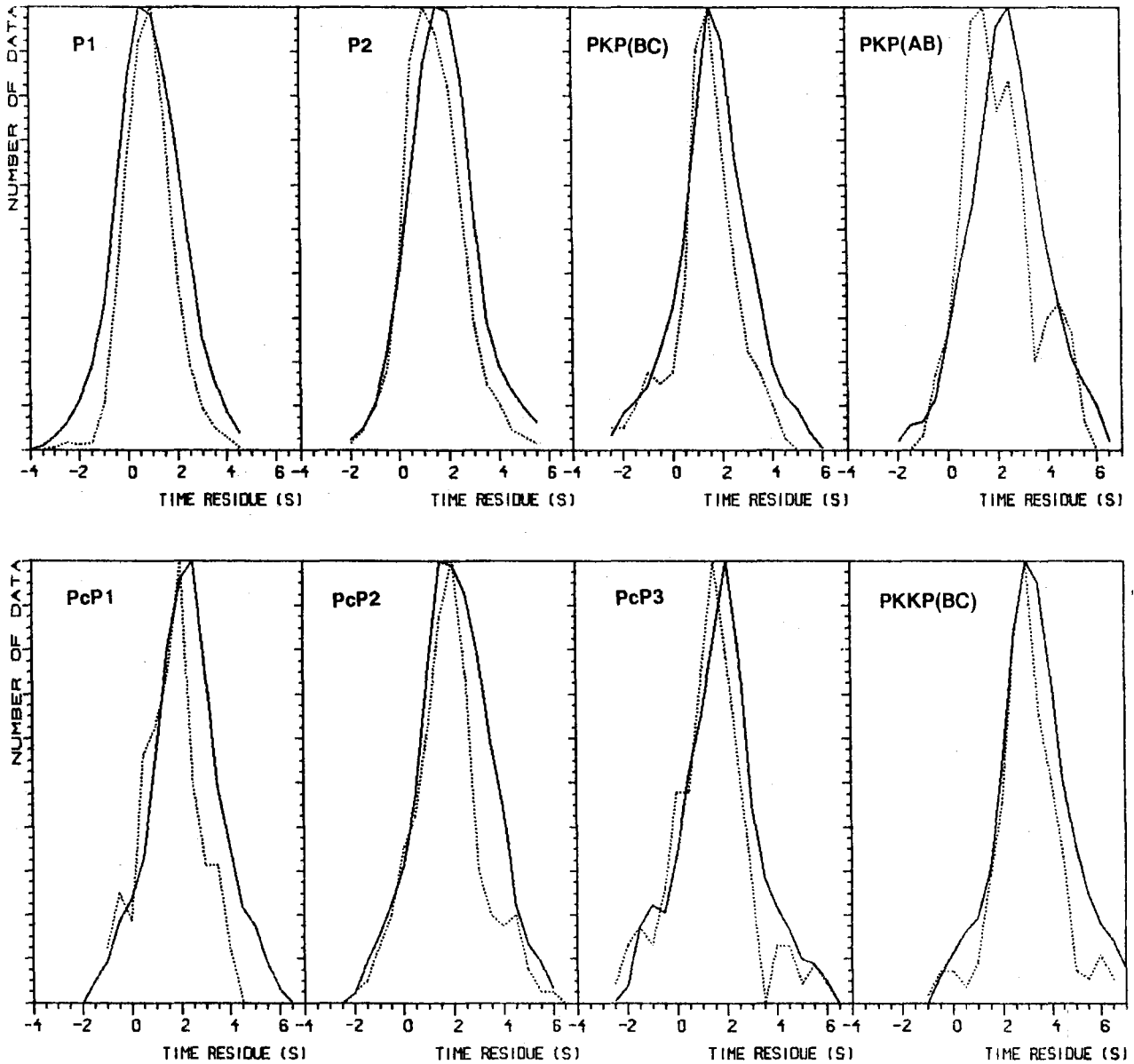
Fig. VII.2.1. Histograms of travel time residuals of 'summary ray'
data. Ray parameter ranges are 2-3 s/d for the BC branches of PKP and
PKKP and for PcP1, 3.5-4 s/d for PcP2 and >4 s/d for the AB branches of
PKP and PnKP and for PcP3. Distance interval for P1 is 65-85°, for P2
85-95°. ————— : all data; ----- : data from deep events (>400 km
depth).
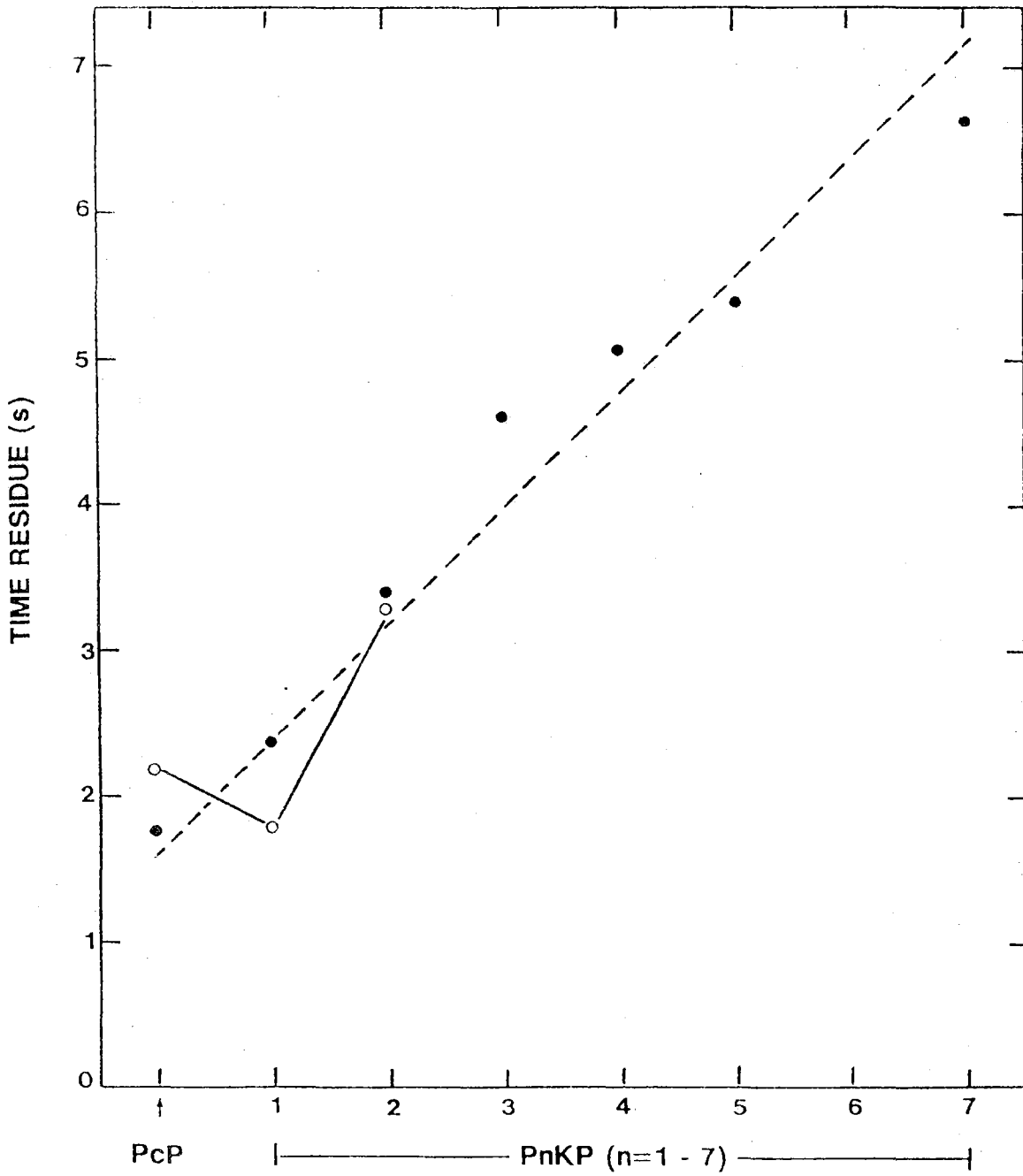
Fig. VII.2.2. Mean 'summary ray' travel time residuals of PcP and PnKP, $n \geq 2$. o: $2 \leq p \leq 3$ s/d; •: $p > 4$ s/d. The dotted line is a linear fit to the data with $p > 4$ s/d.
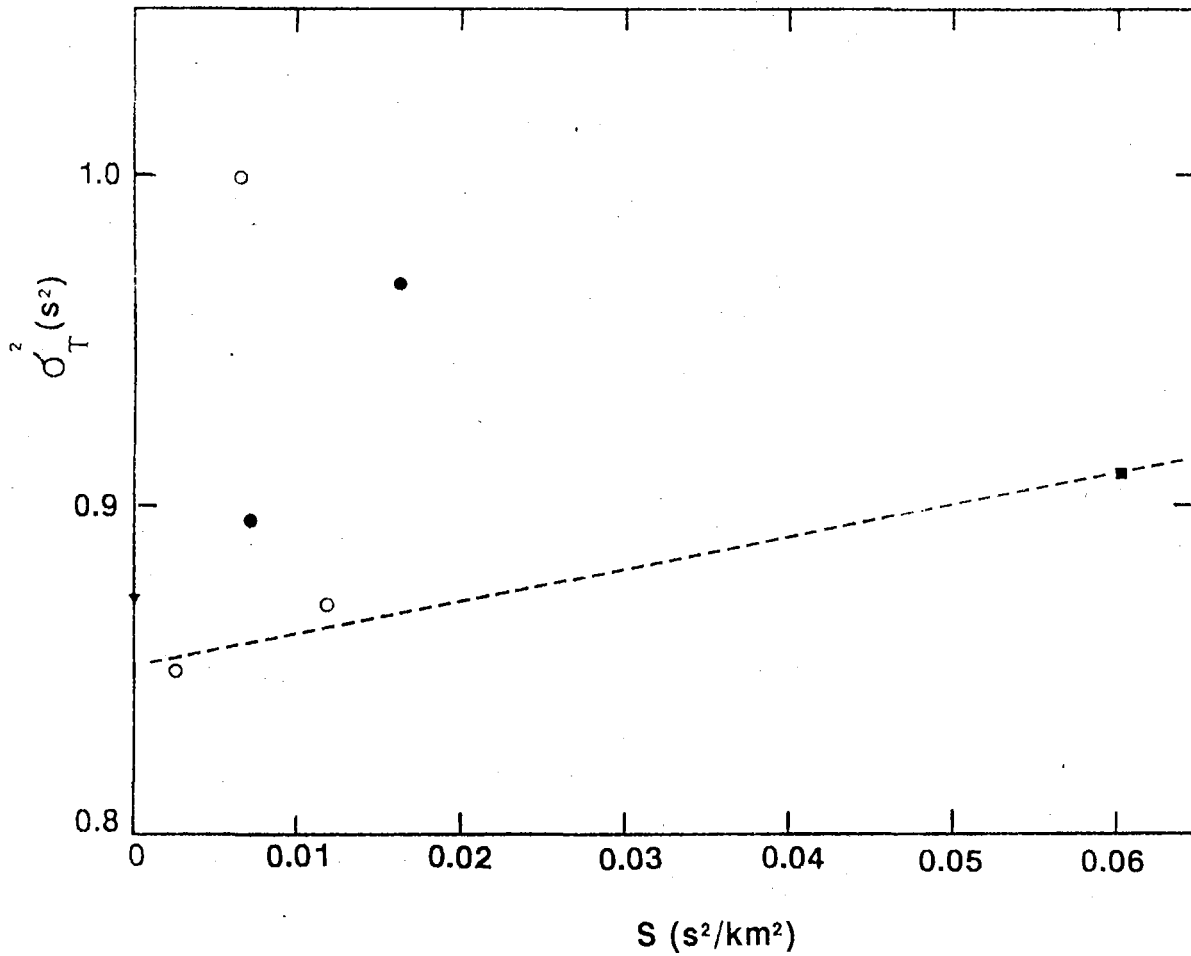
Fig. VII.2.3. Variance σ_T^2 of 'summary ray' travel time residuals, as a function of sensitivity S to boundary topography: $\sigma_T^2 = \sigma_o^2 + S\sigma_r^2$ where σ_r^2 is variance of boundary topography. Data subsets of PcP(o), PKP(●), PKKP(■) and P(▼). The dotted line has a slope $\sigma_r^2 = 1$ km².